



# Irinotecan-Induced Mucositis Is Associated with Goblet Cell Dysregulation and Neural Cell Damage in a Tumour Bearing DA Rat Model

Daniel Thorpe<sup>1</sup> · Ross Butler<sup>1</sup> · Masooma Sultani<sup>2</sup> · Barbara Vanhoecke<sup>3</sup> · Andrea Stringer<sup>1</sup>

Received: 12 January 2018 / Accepted: 19 March 2019 / Published online: 28 March 2019  
© Arányi Lajos Foundation 2019

## Abstract

Irinotecan-induced mucositis is a major oncological problem. Goblet cells secrete mucus, protecting the intestinal mucosa, with secretion altered during mucositis. The enteric nervous system is involved in regulating gut motility and secretion. The aim of this study was to determine whether enteric neural cells and goblet cells are altered following irinotecan treatment. Tumour-bearing Dark Agouti rats were administered a single dose of 175 mg/kg of irinotecan intraperitoneally and 0.01 mg/kg atropine subcutaneously. Experimental and untreated control rats were killed at times 6, 24, 48, 72, 96 and 120 h after treatment. Jejunum and colon samples were formalin fixed. Haematoxylin and eosin staining, Alcian Blue-PAS staining, and immunohistochemistry with S-100 antibody (neural cell marker) were carried out. Statistical analyses were carried out using Kruskal-Wallis test with Dunns post test, Mann Whitney U test and nonlinear regression. Total goblet cells decreased at 72 h compared with controls in the colon ( $p < 0.05$ ). The percentage of cavitated goblet cells decreased compared to all other time points at 120 h in the colon. The number of S-100 positive cells in the submucosal plexus decreased in the colon ( $p = 0.0046$ ) and in the myenteric plexus of the jejunum and colon ( $p = 0.0058$  and  $p = 0.0022$ , respectively), when comparing treated with control. Enteric ganglia in the myenteric plexus of the jejunum decreased at 24 h and 96 h. Irinotecan-induced mucositis is associated with increases in mucus secretion, and enteric neural cell change. These changes may contribute to the pathophysiology of mucositis through the dysregulation of neural signalling.

**Keywords** Mucositis · Chemotherapy · Enteric nervous system · Mucus

✉ Daniel Thorpe  
Daniel.thorpe@unisa.edu.au

Ross Butler  
ross.butler@unisa.edu.au

Barbara Vanhoecke  
cmet@ugent.be

Andrea Stringer  
andrea.stringer@unisa.edu.au

<sup>1</sup> School of Pharmacy and Medical Sciences, University of South Australia, Adelaide 5001, Australia

<sup>2</sup> School of Medical Sciences, Adelaide University, South Australia, Adelaide 5001, Australia

<sup>3</sup> Center for Microbiology Ecology and Technology, University of Ghent, Ghent, Belgium

## Introduction

Gastrointestinal (GI) mucositis is a severe, dose-limiting, toxic side effect of cancer treatment, occurring in more than 40% of cancer patients receiving standard dose chemotherapy and in 100% of cancer patients receiving high dose chemotherapy [1–3]. Symptoms include ulceration, abdominal pain, nausea, vomiting, abdominal bloating and diarrhoea, [2, 4, 5] and often lead to dose reductions, which may result in reduced survival [6, 7]. Furthermore, nutritional adjuncts may be required including fluid replacement, liquid diets and total parenteral nutrition, translating to a substantial cost increase per cycle of chemotherapy [7, 8]. Currently, there is no effective treatment for GI mucositis. However, with continued research to improve the understanding of the pathobiology of mucositis, new possibilities continue to be developed [9–15].

It is now recognised that mucositis is a multifactorial process, with multiple signalling pathways and processes contributing, including both mucosal and luminal modifications to the intestine [16]. Expression and secretion of mucins (high molecular weight acidic glycoproteins secreted by goblet cells) have previously been shown to be associated with mucositis [17–21]. Mucins, as part of the mucus layer, mediate between the luminal contents and the mucosa, protecting the mucosa from bacterial overgrowth and penetration, and digestion, and also by providing attachment sites for commensal bacteria [22–24].

Mucin expression and secretion may be regulated by the enteric nervous system (ENS) [22]. The ENS is considered part of the peripheral nervous system (PNS), and consists of sensory neurons, interneurons and motor neurons [23]. Sensory neurons detect chemical and mechanical stimuli, whilst interneurons transmit data to motor neurons, effecting smooth muscle contraction, distension, and secretion [23]. Therefore, damage to the ENS may significantly affect intestinal homeostasis, either through impaired detection of stimuli, inadequate delivery of information or a compromised ability to respond to stimuli. The mechanisms of mucin regulation are largely unknown. However, enteric neurotransmitters vasoactive intestinal polypeptide (VIP) and nitric oxide (NO) have been shown to be involved in mucin secretion, which may suggest ENS involvement [24, 25]. Therefore this study aims to determine whether irinotecan alters mucin secretion, and if enteric neural cells are damaged during GI mucositis induced by irinotecan.

## Methods

### Ethics

Approval for the use of animals was granted by the Animal Ethics Committees of the Institute of Medical and Veterinary Science (IMVS) and the University of Adelaide, and complied with the National Health and Medical Research Council (Australia) Code of Practice for Animal Care in Research and Teaching (2004) (M-2010-118A). Rats were monitored four times daily, with rats showing a dull ruffled coat with accompanying dull and sunken eyes, cold to touch with no spontaneous movement and a hunched appearance; or a tumour burden greater than 10% of body weight were euthanized.

### Tumour Preparation

The Dark Agouti mammary adenocarcinoma (DAMA) model applied in this study has been used extensively, as previously described [26–29]. Briefly, excised tumours were diced, homogenised and filtered through sterile gauze. The tumour suspension was centrifuged at 1100 rpm for 3 min and

resuspended in sterile phosphate buffered saline (PBS) three times. A viable cell count was carried out using 0.4% v/v trypan blue.

## Experimental Design

All experiments were carried out in inbred female DA rats, weighing between 150 g and 170 g. The rats were single-housed in an animal facility regulated at  $22 \pm 1$  °C and subject to a 14:10 h light-dark cycle. All rats received tumour inoculum of  $4.0 \times 10^6$  cells in 0.5 mL sterile PBS subcutaneously into each flank. Tumours were allowed to grow for 10 days prior to rats receiving irinotecan.

Rats were randomly assigned to groups representing time following irinotecan. The final numbers able to be used for analysis were: control (6), 6 h (5), 24 h (5), 48 h (5), 72 h (8), 96 h (5), 120 h (6). Each experimental rat received 0.01 mg/kg of atropine (to reduce the cholinergic reaction) followed by 175 mg/kg irinotecan intraperitoneally (ip). Six control rats received sorbitol lactic acid buffer (45 mg/ml sorbitol, 0.9 mg/ml lactic acid, pH 3.4) and atropine.

Irinotecan (supplied by Pfizer, Kalamazoo, Michigan, USA) was administered in a sorbitol lactic acid buffer, required for activation of the drug, at time designated 0 h. Rats were killed at the specific time points (with 1 control per time point) using deep anaesthesia with 3% isoflurane in 100% O<sub>2</sub>, followed by exsanguination and cervical dislocation.

The GI tract (pyloric sphincter to the rectum) was dissected out and separated into the small intestine (pyloric sphincter to ileocaecal sphincter) and colon (ascending colon to rectum). Each was flushed with chilled, sterile isotonic saline, prior to 1 cm samples being taken from jejunum and colon.

### Histopathology

All samples were fixed in 10% neutral buffered formalin, processed and embedded in paraffin for histological analysis. Routine haematoxylin and eosin staining was used to observe histopathological changes. Individual parameters of villous blunting, villous fusion (SI) and crypt ablation (SI and colon) were analysed visually based on 10 fields of view. Scoring for villous blunting, crypt ablation was based on the amount of the villi blunted or crypt ablated respectively compared to normal tissue. Villous fusion scoring was based on the percentage of fused villi compared to normal tissue. Inflammatory infiltrate was based on the severity of inflammatory infiltrate present, by ranking each sample then determining the increase in severity compared to the normal tissue. This data was then graded from 0 to 3, with 0 = no change from standard histological structure, 1 = up to one third of tissue affected, 2 = between one and two thirds of tissue affected, and 3 = greater than two thirds of tissue affected.

## Analysis of Goblet Cells

Goblet cells and mucins were analyzed using Alcian Blue/PAS staining. Briefly, sections were dewaxed in xylene and rehydrated through a graded series of ethanol, and stained in Alcian Blue (1% Alcian Blue 8GX, CI 74240, Sigma-Aldrich, in 3% glacial acetic acid, Sigma-Aldrich) for 5 min. Sections were then rinsed in distilled water and oxidized in 1% periodic acid before washing. Sections were then treated for 15 min in Schiff's reagent and washed for 7 min in running tap water. Sections were then dehydrated, cleared and mounted and were analyzed under 20X magnification. Total goblet cell number, and cavitated goblet cell number (recognized by apical indentation into the intracellular store of mucus granules, representative of accelerated mucus secretion by compound exocytosis) [30], in a minimum of 15 complete villi and crypts were counted for each section. Composition of goblet cells was also recorded, with blue staining representative of acidic mucins, magenta staining representative of neutral mucin, and purple staining representative of mixed mucins.

## Immunohistochemistry

To investigate whether the ENS is affected by chemotherapy, anti-S100 antibody (Dako, Denmark, Glostrup) was used. This antibody has previously been shown to detect all neural cells (neurons, glial cells and Schwann cells) of the PNS, and S100A1, S100A6 and S100B [31]. Sections were cut at 10  $\mu$ m, placed onto silane-coated slides (HD Scientific, Sydney, New South Wales, Australia) and heated to 60 °C for 2 h on a heating block. Slides were dewaxed in xylene, and rehydrated through a graded series of ethanol and distilled water, followed by PBS. Endogenous peroxidases were blocked with 3% hydrogen peroxide in methanol for 1 min. Non-specific antibody binding was blocked with blocking solution (Ultra Streptavidin HRP kit, Signet, Dedham, Massachusetts, U.S.A) for 30 min. After washing in PBS, endogenous avidin and biotin were blocked using the Avidin and Biotin kit (Vector Laboratories, Burlingame, California, U.S.A.). Polyclonal rabbit anti-S100 antibody (Dako, 1:800 dilution) was then applied for 30 min at room temperature (RT). After washing in PBS (3  $\times$  5 min), linking reagent (Ultra Streptavidin HRP kit) was applied for 30 min, followed by washes in PBS (3  $\times$  5 min). Labelling reagent (Ultra Streptavidin HRP kit) was then applied for 30 min then washed in PBS (3  $\times$  5 min). Staining was visualised using 3,3'-diaminobenzidine (DAB) and counterstained using Lillie Mayer's Haematoxylin, before dehydrating, clearing and cover slipping. A cell count of stained cells was carried out over 1 mm lengths of tissue, with nerve bundles (groups of 4 or more stained cells) and axons and neural cells (less than 4 stained cells) counted and recorded, as well as the

location of the cells. Staining intensity was also graded to analyse the change in expression, where 0 = negative; 1 = weak; 2 = moderate; 3 = strong; 4 = very intense, based on a previously validated technique [32].

## Statistical Analysis

Statistical analysis was performed using a Kruskal-Wallis test for non-parametric data with a secondary Dunn's comparative test for multiple group comparisons, and Mann Whitney U test for comparing two groups only using GraphPad Prism 5.0 software (Graphpad software, California, U.S.A). Non-parametric linear regression was also carried out to determine if a correlation between histological damage, goblet cell, and nerve cell parameters exists using StataC12 (StataCorp LP, Texas, USA). Differences between mean ranks were determined to be significant at  $p < 0.05$ . Cohen's D tests to determine clinical significance were also carried out as a measure of effect size. The effect was considered small if  $d > 0.20$ , moderate if  $d > 0.50$ , and large if  $d > 0.80$  [33].

## Results

### Irinotecan Causes Histopathological Damage in the Intestine

Histological changes were observed along the GIT following irinotecan administration (Fig. 1), as previously described [34, 35]. In the jejunum, villous fusion and blunting increased between 24 and 120 h following irinotecan. Crypt ablation was greatest at 24 and 48 h following irinotecan, with crypt hypoplasia evident at 96 h. In the colon, crypt ablation increased from 6 to 96 h following irinotecan (Fig. 1). No effects on tumour growth were observed (data not shown).

### Irinotecan Modifies Goblet Cell Number and Composition

#### Composition

Alcian Blue/PAS staining showed the composition of mucins in goblet cells in the jejunum was mixed (purple) and neutral (magenta) in control rats. The composition changed between 24 and 48 h following irinotecan, with increased acidic (blue) mucins present. In the colon, composition of mucins in goblet cells was predominantly mixed in control rats. The composition of mucins change from mixed to neutral following irinotecan, becoming neutral at 120 h (Fig. 2).

**Fig. 1** Histopathological changes in the jejunum and colon of irinotecan-treated rats compared with vehicle controls. **a** Jejunum: villous fusion and blunting, and crypt ablation increased following irinotecan. At 48 h an arrow highlights villous blunting, at 96 h another arrow highlights villous fusion. **b** Colon: crypt ablation increased following irinotecan. At 72 h an arrow highlights crypt ablation. (Original magnifications 20X) **c** Pathology scores of villous fusion in the jejunum following irinotecan. **d** Pathology scores of villous blunting in the jejunum following irinotecan. **e** Pathology scores of crypt ablation in the jejunum following irinotecan. **f** Pathology scores of crypt ablation in the colon following irinotecan

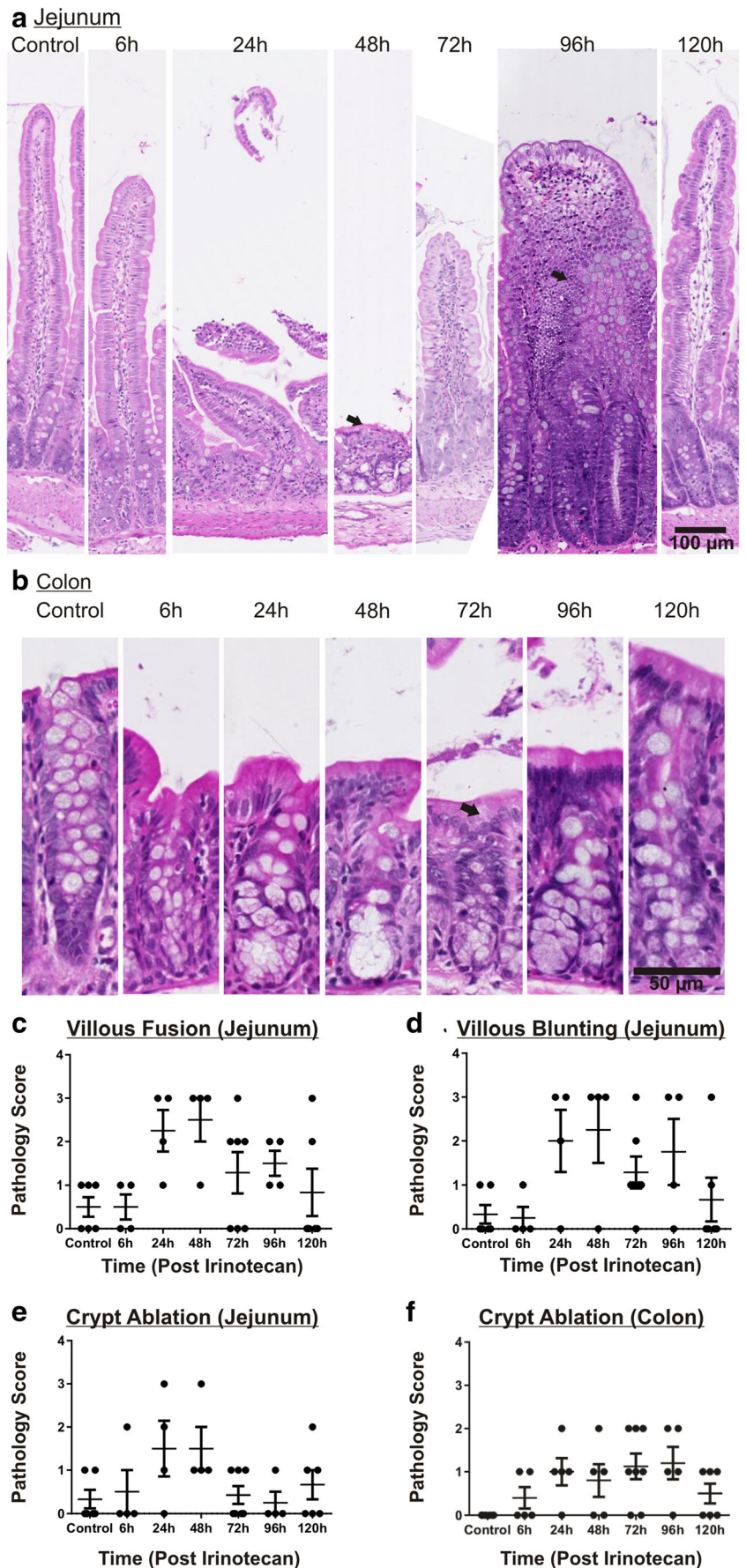
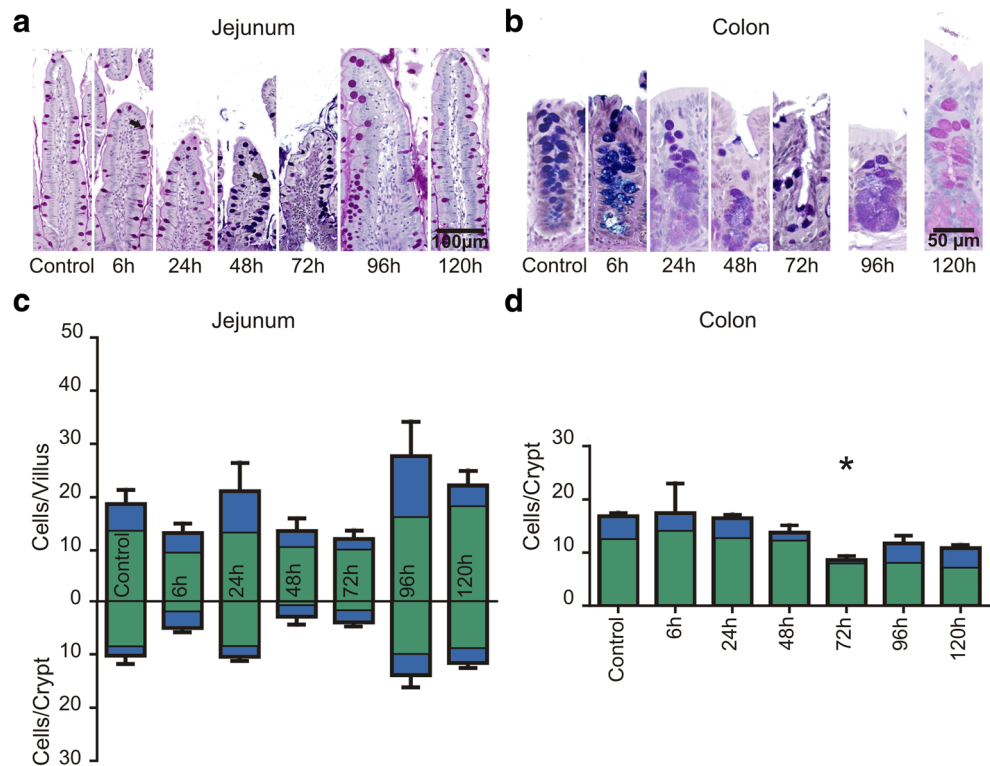


**Fig. 2** Alcian Blue-PAS staining of changes in the jejunum and colon of irinotecan-treated rats compared with vehicle controls. **a** Jejunum **(b)** Colon (Original Magnification 20X). **c** Counts of intact (green) and cavitated (blue) goblet cells in the jejunum in the villus and crypts after irinotecan administration. **d** Counts of intact (green) and cavitated (blue) goblet cells in the colon in the crypts after irinotecan administration. (\* Denotes statistical significance, where  $p < 0.05$ )



### Quantification of Goblet Cells

Mean total goblet cell numbers were  $18.7 \pm 2.6$  (mean  $\pm$  SEM) per villus and  $10.3 \pm 1.4$  per crypt in the jejunum of control rats. Mean total goblet cells were lowest at 6 h ( $13.2 \pm 1.8$  and  $5.1 \pm 0.6$ , villus and crypt, respectively), 48 h ( $13.7 \pm 2.3$  and  $2.9 \pm 1.5$ ) and 72 h ( $12.2 \pm 1.5$  and  $4.0 \pm 0.8$ ), when histological damage was also present. Goblet cell numbers were greatest (not significant) at 96 h ( $27.7 \pm 6.4$  and  $13.9 \pm 2.1$ , villus and crypt, respectively) following irinotecan. The mean ranks of the total number of goblet cell numbers per villus and crypt both deviated significantly across time points ( $p = 0.043$  and  $p = 0.0003$ , respectively) (Fig. 2). Comparisons between individual time points did not reach significance.

Mean total goblet cell numbers in the colon of control rats were  $16.8 \pm 0.9$  per crypt (mean  $\pm$  SEM). Mean total goblet cells per crypt decreased following irinotecan, with the lowest number at 72 h ( $8.6 \pm 1.1$ ). The mean ranks of the total number of goblet cells per crypt deviated significantly ( $p = 0.0061$ ) at 72 h following irinotecan compared with control (mean rank difference 21.0) (Fig. 2).

**Cavitated Goblet Cells** The percentage of cavitated goblet cells (of total goblet cells) in the jejunum of control rats was  $80.9 \pm 5.5$  per villus and  $77.6 \pm 3.2$  per crypt. The percentage of cavitated goblet cells per villus was greatest at 72 h ( $85.7 \pm 3.1$ , Cohen's  $D = 2.1$ , large effect) and was lowest at 24 h ( $66.1 \pm 7.1$ , Cohen's  $D = 0.5$ , small effect) following irinotecan. In the

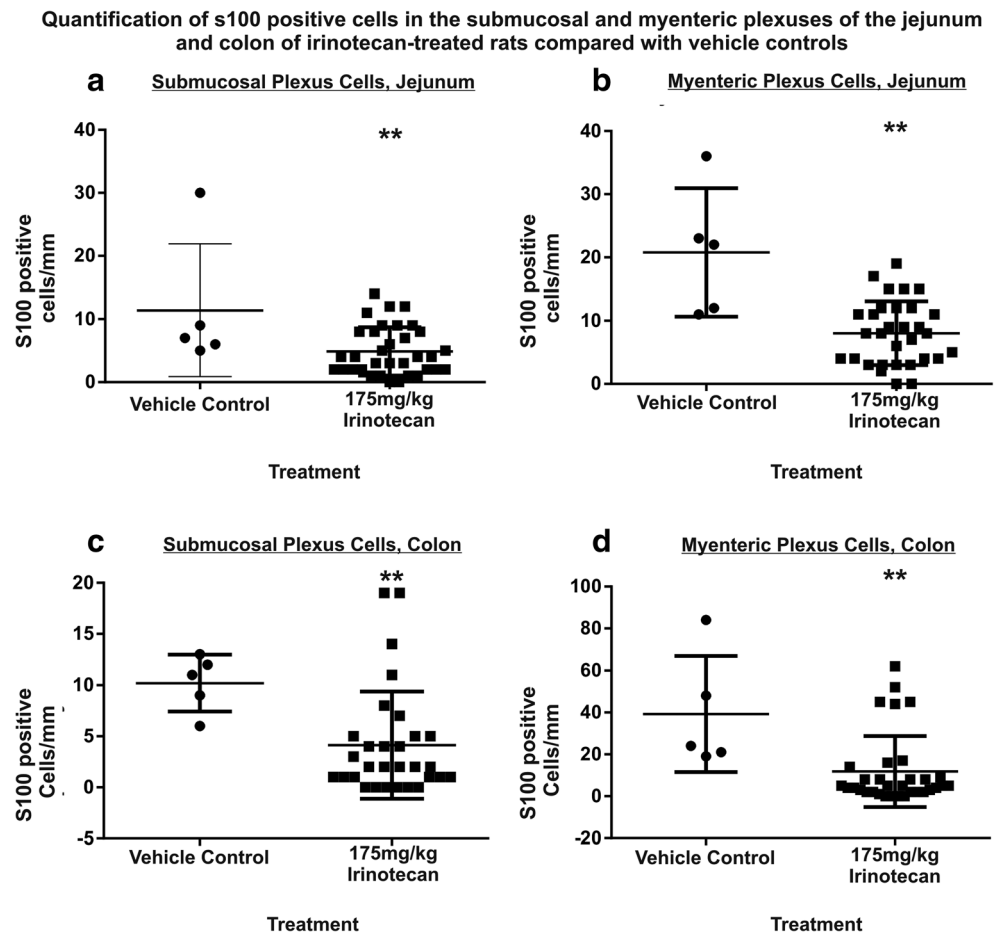
crypts, the percentage of cavitated goblet cells was highest at 72 h ( $93.2 \pm 2.3$ , Cohen's  $D = 1.4$ , large effect) and lowest at 120 h ( $75.5 \pm 3.1$ , Cohen's  $D = 0.9$ , large effect). The mean ranks of the percentage of cavitated cells in the villi did not deviate significantly. In contrast, the percentage of cavitated cells in the crypts of the jejunum of irinotecan-treated rats deviated significantly across time points ( $p = 0.018$ ), although individual time point comparisons did not reach significance.

In the colon, the percentage of cavitated goblet cells (of total goblet cells) in control rats was  $71.31 \pm 6.38$  of total goblet cells per crypt (Fig. 3). The percentage of cavitated goblet cells was highest at 48 h following irinotecan ( $89.9 \pm 3.5$ , Cohen's  $D = 0.6$ , moderate effect), and lowest at 120 h ( $46.2 \pm 7.8$ , Cohen's  $D = 2.9$ , large effect) (Fig. 3). The mean ranks deviated significantly across all time points ( $p = 0.033$ ), although individual time point comparisons did not reach significance (Fig. 2).

### Immuno-Labeling of S100 Positive Cells

S100 (a marker for neurons, glial cells and Schwann cells of the PNS) was analysed in the submucosal plexus and myenteric plexus of the jejunum and colon. The mean staining intensities of S100 positive cells of vehicle control rats in the jejunum was  $1.3 \pm 0.5$  (mean  $\pm$  SEM) and  $4.0 \pm 0.0$  for S100 positive cells (including neurons and glial cells) and enteric ganglia, respectively. Mean staining intensity of vehicle control rats in the colon was  $2.5 \pm 0.7$  and  $1.0 \pm 0.3$  for S100

**Fig. 3** Quantification of S100 positive cells in the submucosal and myenteric plexuses of the jejunum and colon of irinotecan-treated rats compared with vehicle controls (a) Jejunum, submucosal plexus. b Jejunum, myenteric plexus. c Colon, submucosal plexus. d Colon, myenteric plexus. (\*\*Denotes statistical significance, where  $p < 0.05$ )



positive cells and enteric ganglia, respectively. Following irinotecan administration, the staining intensity significantly decreased in the colon at 72 h ( $0.3 \pm 0.2$ ,  $d = 2.6$ , large effect) ( $p < 0.05$ ) (Fig. 3).

## Quantification of Neural Cells

### Neural Cells

The mean number of S100 positive cells in the submucosal plexuses of the jejunums of vehicle control rats was  $11.4 \pm 4.7$  per millimetre (mm) length. The mean ranks of the number of S100 positive cells per mm did not deviate significantly following irinotecan (data not shown). However, the number of S100 positive cells present in the submucosal plexus decreased significantly in irinotecan treated rats ( $p = 0.01$ ) when all irinotecan treated rats were compared to vehicle controls, irrespective of time point (Fig. 4).

The mean number of S100 positive cells in the myenteric plexuses of the jejunums of vehicle control rats was  $20.80 \pm 4.53$  per mm length. The number of S100 positive cells was lowest at 24 and 48 h ( $7.0 \pm 1.7$ , and  $7.0 \pm 1.6$ , respectively,  $d = 2.4$  and  $2.4$ , respectively, large effects) following irinotecan.

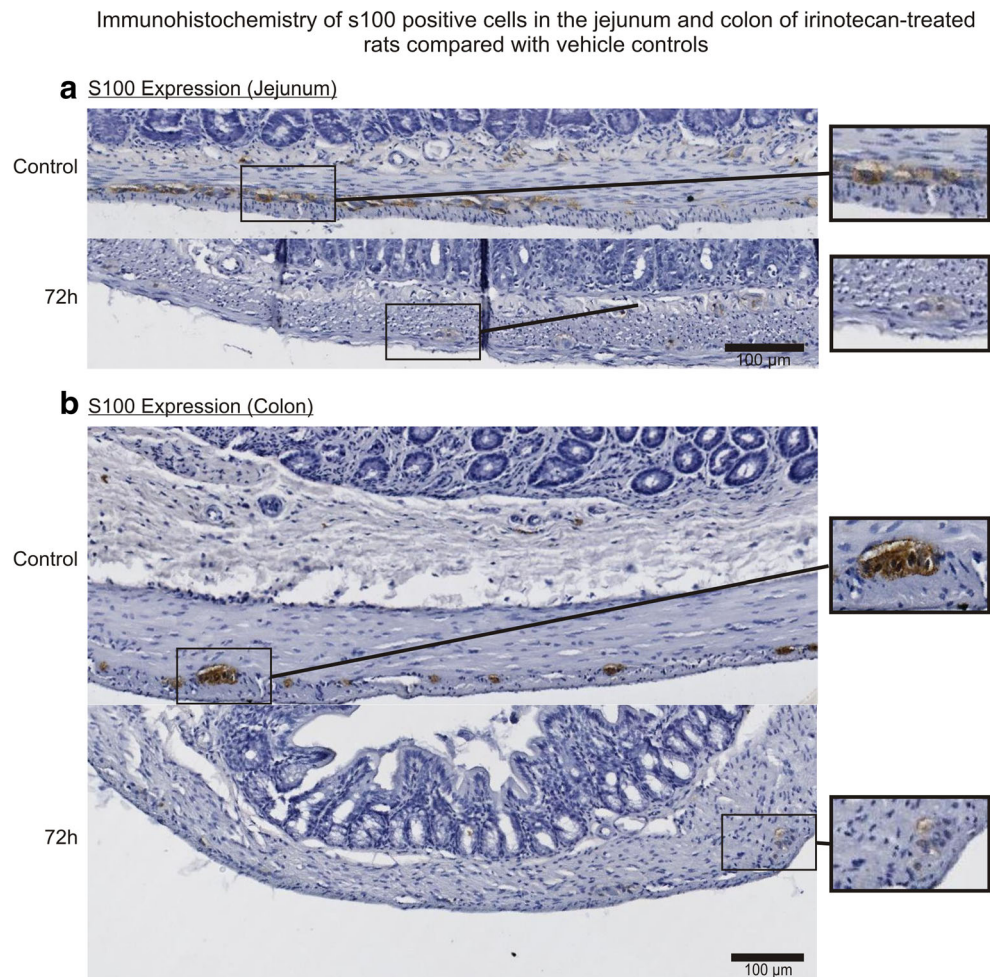
The mean ranks of S100 positive cells per mm did not deviate significantly across individual groups (data not shown). However, the number of S100 positive cells present in the myenteric plexus decreased significantly in irinotecan treated rats ( $p = 0.0058$ ) when all irinotecan treated rats were compared with vehicle controls, irrespective of time point (Fig. 4).

The mean numbers of S100 positive cells in the submucosal and myenteric plexuses of the colons of vehicle control rats were  $10.2 \pm 1.2$  and  $39.2 \pm 12.4$  per mm, respectively. This number was lowest at 72 h following irinotecan treatment in the submucosal plexuses ( $2.1 \pm 2.6$  per mm,  $d = 1.8$ , large effect) and at 120 h in the myenteric plexuses ( $4.0 \pm 3.5$  per mm,  $d = 2.1$ , large effect). Mean ranks of S100 positive cells per mm did not deviate significantly between individual time points for both regions (data not shown). However, the number of S100 positive cells per mm was significantly lower in treated rats ( $p = 0.0046$  and  $0.0022$ , respectively) when all irinotecan treated rats were compared with vehicle control rats (Fig. 4).

### Enteric Ganglia

The mean number of enteric ganglia in the jejunum of vehicle control rats was  $4.2 \pm 1.2$  (mean  $\pm$  SEM) per mm. The lowest

**Fig. 4** Immunohistochemistry of S100 positive cells in the jejunum and colon of irinotecan-treated rats compared with vehicle controls. **a** Immunohistochemistry of S100 positively stained cells in the jejunum. **b** Immunohistochemistry of S100 positively stained cells in the colon. Insets = Enteric ganglia; Original magnification 20X



numbers of enteric ganglia were present at 24 h ( $1.8 \pm 0.8$  per mm). There was no significant difference between irinotecan treated and vehicle control rats, mean ranks of the number of nerve bundles per mm did not deviate significantly, and effect size was not significant (data not shown).

The number of enteric ganglia in the colon of vehicle control rats was  $6.3 \pm 2.4$  (mean  $\pm$  SEM) per mm. There was no significant difference between irinotecan treated and vehicle control rats, mean ranks of the number of enteric ganglia did not deviate significantly, and effect size was not significant (data not shown).

### Association of Goblet Cell Parameters with Neural Cells in the Intestine

Non-parametric regression analysis was carried out to determine associations between experimental parameters. In the jejunum, crypt cavitated goblet cells and myenteric plexus nerve bundles were strongly inversely correlated (pseudo  $R^2 = 0.16$ ). In the colon, cavitated goblet cells and submucosal

nerve bundles in the colon were strongly correlated (Pseudo  $R^2 = 0.08$ ) (Table 1, Fig. 5).

### Discussion

GI mucositis is a severe, dose-limiting, toxic side effect of cancer treatment [7, 8]. This study has demonstrated for the first time that the ENS may be involved in irinotecan-induced mucositis, potentially through regulation of goblet cell secretion. Previous studies in rat models for chemotherapy-induced mucositis have demonstrated that goblet cells and mucins are significantly affected by chemotherapy agents 5-FU and irinotecan [18, 19]. However, these studies have been performed using non-tumour bearing rats, and did not investigate the ENS in the pathobiology of mucositis.

The findings of this study are consistent with previous published results using irinotecan. Specifically, this study has shown total goblet cell numbers in the jejunum and colon decreased between 48 and 72 h, and 72 h respectively following irinotecan administration, consistent with previous studies

**Table 1** Non-parametric regression analyses of goblet cell and enteric nervous system variable parameters during mucositis

Gut Region	Dependent variable	Independent variable	Coefficient	95% CI coefficient	Pseudo R <sup>2</sup>
Jejunum	Crypt Cavitated goblet cells	Myenteric Plexus, Enteric Ganglia	-1.05	-2.10 -0.005	0.16
Colon	Crypt, Cavitated Goblet cells	Submucosal Plexus, Enteric Ganglia	2.87	0.04 5.69	0.08

by Stringer and colleagues [36]. In this study, we demonstrate, for the first time, associations between different parameters of GI damage following irinotecan administration, mucin secretion by goblet cells (suggestive of changes in barrier function), and decreases in S100 expression, which may suggest loss of enteric neurons or glial cells.

This study also demonstrates temporal differentiation of GI damage between the jejunum and colon following irinotecan, with crypt ablation beginning simultaneously in the jejunum and colon, but with recovery completed earlier in the jejunum (48 h) compared to the colon (96 h).

This is consistent with the model for alimentary mucositis, as local variations in specialization for specific function lead to differences in manifestation of mucositis (Keefe [4]). This is supported by previous studies. In an irinotecan-induced female dark agouti rat mucositis model (0.01 mg/kg subcutaneous atropine, 200 mg/kg irinotecan in 45 mg/ml of sorbitol/0.9 mg/ml lactic acid, pH 3.4), crypt length decreased later in the colon compared to the jejunum (Logan et al. [34]). This differentiation between the jejunum and colon in irinotecan models may be the result of the excretion pathway of irinotecan. Irinotecan is excreted (as inactive metabolite SN-38G) following processing in the liver via bile, which is then delivered to the small intestine via the bile duct. At this point, intestinal bacteria located in the jejunum that produce bacterial  $\beta$ -glucuronidase have the capacity to convert the inactive SN38G back to the active (and damage causing) SN-38

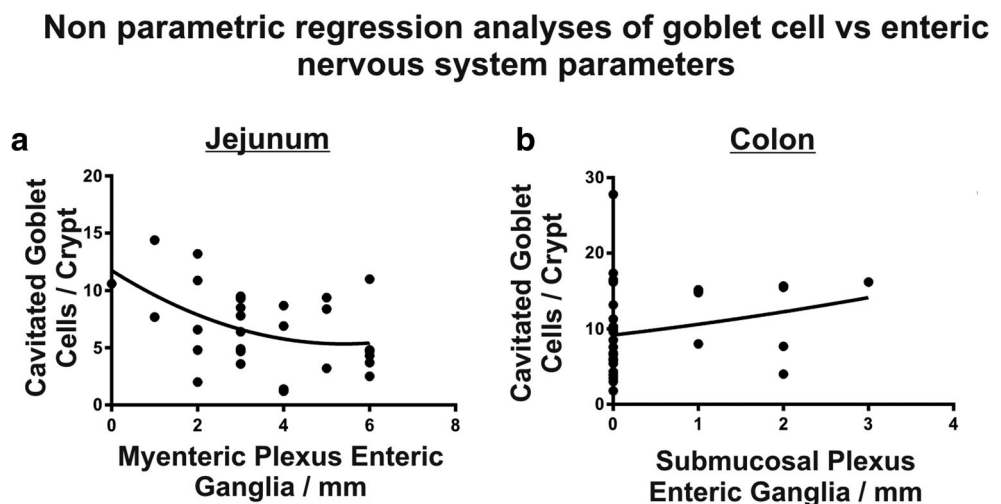
[37–39]. SN-38 has the capacity to initiate more intestinal damage as it travels through the small and then the large intestine, and may explain the timeline of damage observed.

Goblet cell composition was also altered during mucositis with the jejunum becoming more acidic and the colon becoming more neutral. This may have to effects on the intestine. Firstly, neutral mucins buffer the mucosa from an acidic environment [40, 41]. Secondly, the microbiome may be altered due to changes in mucous composition as previous research has demonstrated bacterial colonisation can be dependent on mucin pH [42].

Goblet cell numbers were also shown to vary following irinotecan, in the jejunum and colon. The percentage of cavitated goblet cells in the jejunum, in the crypts was highest at 72 h in the jejunum, and the total goblet cell numbers was lowest in the jejunum between 48 and 72 h. However, in the colon crypts the percentage of cavitated cells did not change significantly. The total number of goblet cells was significantly ( $p < 0.05$ ) decreased compared to controls at 72 h, and may have been the result of variations in local functions subsequent to histological damage, or variations in ligands associated with goblet cell exocytosis, such as VIP [25, 43], NO generations [24, 25, 44] and dimethyl-PGE2 [25, 45].

[40–42] Indirect damage also occurs through initiation of damage-related signalling pathways, resulting in production of pro-inflammatory cytokines and apoptosis promoters in the intestine [34, 46]. Interleukin (IL)-1, IL-4, IL-6 and IL-9, and tumour necrosis factor (TNF)- $\alpha$  (pro-inflammatory

**Fig. 5** Non parametric regression analyses of goblet cell vs enteric nervous system parameters. **a** Jejunum, cavitated goblet cells per crypt and myenteric plexus enteric ganglia per mm. **b** Colon, cavitated goblet cells per crypt and submucosal plexus enteric ganglia per mm



cytokines), cholinergic stimulation, and intestinal anaphylaxis are also involved in rapid goblet cell exocytosis [47–50]. Further investigation into the process of goblet cell exocytosis following irinotecan is warranted, and may provide targets for agents to maintain the protective barrier to restrict damage to the underlying tissue.

The increased percentage of cavitation of goblet cells in the crypts of the jejunum and colon following irinotecan may suggest that mucus secretion is enhanced in the crypts during mucositis, or is the result of direct damage to epithelial cells occurring early following chemotherapy. It may also be representative of stimulation of exocytosis of goblet cells by pro-inflammatory cytokines [50], which are known to be released during mucositis [46].

Goblet cell numbers were also shown to vary following irinotecan between the jejunum and colon. The percentage of cavitated goblet cells in the jejunum crypts was highest at 72 h, whilst the total goblet cell numbers were lowest in the jejunum at 48–72 h. In the colon crypts the percentage of cavitated cells did not change significantly. However, the total number of goblet cells significantly ( $p < 0.05$ ) decreased compared to controls at 72 h, and may be the result of variations in local functions from the altered histology, or variations in ligands associated with goblet cell exocytosis, such as VIP [25, 43], NO generations [24, 25, 44] and dimethyl-PGE2 [25, 45]. It is possible that variations in inflammation or variations in the enteric nervous system in the jejunum and colon may cause differences in the pathophysiology of mucositis between the jejunum and colon.

Expression of the neural marker S100 decreased following irinotecan administration, with fewer neural cells stained in the jejunum and colon, most notably in the myenteric plexus. As the data generated from this study did not allow differentiation between neural cell types, any decreases in neurons could have been sensory neurons, interneurons, or motor neurons, or combinations of these. Sensory neuron loss would affect the ability to detect chemical and mechanical stimuli, impacting potential pH buffering and digestive processes [51, 52]. Loss of interneurons would affect transmission of sensory and chemical data detected by receptors for processing, and to effector motor neurons [51, 52]. Motor neuron depletion would affect smooth muscle contraction and distension, and epithelial secretion [51].

The reduced number of neural cells following irinotecan in the myenteric plexus is likely to reduce neural stimulation of circular and longitudinal smooth muscle, affecting mostly motility, and the reduced numbers of neural cells in the submucosal plexus may affect secretory cells. Neural cell alteration in the myenteric plexus may result in reduced smooth muscle contraction (affecting gut motility), and secretion. However, the decrease in total goblet cell numbers may indicate continued exocytosis of mucins, which contradicts the expected reduction in secretogens, which may result from a decreased submucosal

plexus enteric neural cells [43, 53]. An explanation for this may be the increased levels of pro-inflammatory cytokines, which have previously been shown to cause rapid exocytosis of mucins [50]. This dysregulated secretion may be the result of increased pro-inflammatory cytokines, with IL-1, IL-4, IL-6, IL-9 and TNF- $\alpha$  shown to stimulate the rapid release of mucin from goblet cells [50], and also shown to be significantly increased following chemotherapy [46]. The untimely exocytosis of mucin stores is likely to lead to disrupted barrier function. In addition, if glial cells are decreased, this may affect the supportive and conductive functions of the ENS.

The ENS has not yet been investigated extensively in the context of mucositis. However, our data suggests that the ENS may contribute to some of the symptoms of mucositis relating to secretion and motility. Strong inverse correlations were observed between cavitated goblet cells and enteric ganglia in the small intestine, suggesting that dysregulated release of stimuli or neurotransmitters may be occurring in response to irinotecan-induced enteric nerve damage, and may impact on the secretory function of target (goblet) cells. Further *in vitro* investigations of exocytosis of goblet cells stimulated with irinotecan metabolites are warranted, specifically investigating the response to pro-inflammatory cytokines.

Anti-inflammatory cytokines, such as IL-22 (a member of IL-10 family) have been shown to be important in maintaining goblet cell integrity in a mouse model of helminth infection [54]. Anti-inflammatory cytokines are thought to be reduced following chemotherapy [55]. Therefore, if IL-22 is decreased following irinotecan administration, goblet cell integrity may become compromised with the loss of this protective factor. This highlights the need for larger, more detailed *in vitro* and *in vivo* studies of the mechanisms underlying altered goblet cell function, viability, and innervation in response to irinotecan and other chemotherapy agents.

In conclusion, irinotecan-induced mucositis is associated with histopathological damage, goblet cell and enteric nerve cell damage. These phenomena may be the result of inflammatory signalling up-regulated by irinotecan. Damage to goblet cells and enteric nerves is likely to affect secretion and motility during chemotherapy and radiotherapy treatment, potentially resulting in altered intestinal function.

**Funding** This study was funded by NHMRC funding (1016696).

**Compliance with Ethical Standards** Dr. Daniel Thorpe declares that he has no conflict of interest, Ms. Masooma Sultani declares that she has no conflict of interest, Professor Ross Butler declares he has no conflict of interest, Dr. Barbara Vanhoecke declares she has no conflict of interest, and Dr. Andrea Stringer declares that she has no conflict of interest. Furthermore, all applicable international, national, and/or institutional guidelines for the care and use of animals were followed, and all procedures performed in studies involving animals were in accordance with the ethical standards of the institution or practice at which the studies were conducted.

## References

- Keefe DM, Brealey J, Golland GJ, Cummins AG (2000) Chemotherapy for cancer causes apoptosis that precedes hypoplasia in crypts of the small intestine in humans. *Gut* 47(5):632–637
- Keefe DM, Cummins AG, Dale BM, Kotasek D, Robb TA, Sage RE (1997) Effect of high-dose chemotherapy on intestinal permeability in humans. *Clin Sci (Lond)* 92(4):385–389
- Pico JL, Avila-Garavito A, Naccache P (1998) Mucositis: its occurrence, consequences, and treatment in the oncology setting. *Oncologist* 3(6):446–451
- Keefe DM (2004) Gastrointestinal mucositis: a new biological model. *Support Care Cancer* 12(1):6–9. <https://doi.org/10.1007/s00520-003-0550-9>
- Sonis ST, Costa JW Jr, Evitts SM, Lindquist LE, Nicolson M (1992) Effect of epidermal growth factor on ulcerative mucositis in hamsters that receive cancer chemotherapy. *Oral Surg Oral Med Oral Pathol* 74(6):749–755
- Savarese DM, Hsieh C, Stewart FM (1997) Clinical impact of chemotherapy dose escalation in patients with hematologic malignancies and solid tumors. *J Clin Oncol* 15(8):2981–2995
- Elting LS, Cooksley C, Chambers M, Cantor SB, Manzullo E, Rubenstein EB (2003) The burdens of cancer therapy. Clinical and economic outcomes of chemotherapy-induced mucositis. *Cancer* 98(7):1531–1539. <https://doi.org/10.1002/cncr.11671>
- Elting LS, Cooksley CD, Chambers MS, Garden AS (2007) Risk, outcomes, and costs of radiation-induced oral mucositis among patients with head-and-neck malignancies. *Int J Radiat Oncol Biol Phys* 68(4):1110–1120. <https://doi.org/10.1016/j.ijrobp.2007.01.053>
- Gibson RJ, Keefe DM, Lalla RV, Bateman E, Blijlevens N, Fijlstra M, King EE, Stringer AM, van der Velden WJ, Yazbeck R, Elad S, Bowen JM (2013) Systematic review of agents for the management of gastrointestinal mucositis in cancer patients. *Support Care Cancer* 21(1):313–326. <https://doi.org/10.1007/s00520-012-1644-z>
- Lalla RV, Bowen J, Barasch A, Elting L, Epstein J, Keefe DM, McGuire DB, Migliorati C, Nicolatou-Galitis O, Peterson DE, Raber-Durlacher JE, Sonis ST, Elad S (2014) MASCC/ISOO clinical practice guidelines for the management of mucositis secondary to cancer therapy. *Cancer* 120(10):1453–1461. <https://doi.org/10.1002/cncr.28592>
- Keefe DM, Schubert MM, Elting LS, Sonis ST, Epstein JB, Raber-Durlacher JE, Migliorati CA, McGuire DB, Hutchins RD, Peterson DE (2007) Updated clinical practice guidelines for the prevention and treatment of mucositis. *Cancer* 109(5):820–831. <https://doi.org/10.1002/cncr.22484>
- Sonis ST, Elting LS, Keefe D, Peterson DE, Schubert M, Hauer-Jensen M, Bekele BN, Raber-Durlacher J, Donnelly JP, Rubenstein EB (2004) Perspectives on cancer therapy-induced mucosal injury: pathogenesis, measurement, epidemiology, and consequences for patients. *Cancer* 100(9 Suppl):1995–2025. <https://doi.org/10.1002/cncr.20162>
- Rubenstein EB, Peterson DE, Schubert M, Keefe D, McGuire D, Epstein J, Elting LS, Fox PC, Cooksley C, Sonis ST (2004) Clinical practice guidelines for the prevention and treatment of cancer therapy-induced oral and gastrointestinal mucositis. *Cancer* 100(9 Suppl):2026–2046. <https://doi.org/10.1002/cncr.20163>
- Saltz LB (2003) Understanding and managing chemotherapy-induced diarrhea. *J Support Oncol* 1(1):35–46; discussion 38–41, 45–36
- Wadler S, Benson AB 3rd, Engelking C, Catalano R, Field M, Kornblau SM, Mitchell E, Rubin J, Trotta P, Vokes E (1998) Recommended guidelines for the treatment of chemotherapy-induced diarrhea. *J Clin Oncol* 16(9):3169–3178
- Al-Dasooqi N, Sonis ST, Bowen JM, Bateman E, Blijlevens N, Gibson RJ, Logan RM, Nair RG, Stringer AM, Yazbeck R, Elad S, Lalla RV (2013) Emerging evidence on the pathobiology of mucositis. *Support Care Cancer* 21(7):2075–2083. <https://doi.org/10.1007/s00520-013-1810-y>
- de Koning BA, Sluis M, Lindenbergh-Kortleve DJ, Velcich A, Pieters R, Buller HA, Einerhand AW, Renes IB (2007) Methotrexate-induced mucositis in mucin 2-deficient mice. *J Cell Physiol* 210(1):144–152. <https://doi.org/10.1002/jcp.20822>
- Stringer AM, Gibson RJ, Logan RM, Bowen JM, Yeoh AS, Laurence J, Keefe DM (2009) Irinotecan-induced mucositis is associated with changes in intestinal mucins. *Cancer Chemother Pharmacol* 64(1):123–132. <https://doi.org/10.1007/s00280-008-0855-y>
- Stringer AM, Gibson RJ, Logan RM, Bowen JM, Yeoh AS, Hamilton J, Keefe DM (2009) Gastrointestinal microflora and mucins may play a critical role in the development of 5-fluorouracil-induced gastrointestinal mucositis. *Exp Biol Med (Maywood)* 234(4):430–441. <https://doi.org/10.3181/0810-rm-301>
- Saegusa Y, Ichikawa T, Iwai T, Goso Y, Okayasu I, Ikezawa T, Shikama N, Saigenji K, Ishihara K (2008) Changes in the mucus barrier of the rat during 5-fluorouracil-induced gastrointestinal mucositis. *Scand J Gastroenterol* 43(1):59–65
- Verburg M, Renes IB, Meijer HP, Taminiou JA, Buller HA, Einerhand AW, Dekker J (2000) Selective sparing of goblet cells and paneth cells in the intestine of methotrexate-treated rats. *Am J Physiol Gastrointest Liver Physiol* 279(5):G1037–G1047
- Thorpe D, Stringer A, Butler R (2013) Chemotherapy-induced mucositis: the role of mucin secretion and regulation, and the enteric nervous system. *Neurotoxicology* 38:101–105. <https://doi.org/10.1016/j.neuro.2013.06.007>
- Wood JD (2011) Enteric nervous system: the brain-in-the-gut. In: *Integrated systems physiology: from molecule to function to disease*, vol 26. Morgan & Claypool Life Sciences, Ohio
- Branka JE, Vallette G, Jarry A, Laboisie CL (1997) Stimulation of mucin exocytosis from human epithelial cells by nitric oxide: evidence for a cGMP-dependent and a cGMP-independent pathway. *Biochem J* 323(Pt 2):521–524
- Plaisancie P, Barcelo A, Moro F, Claustre J, Chayvialle JA, Cuber JC (1998) Effects of neurotransmitters, gut hormones, and inflammatory mediators on mucus discharge in rat colon. *Am J Phys* 275(5 Pt 1):G1073–G1084
- Gibson RJ, Keefe DM, Thompson FM, Clarke JM, Golland GJ, Cummins AG (2002) Effect of interleukin-11 on ameliorating intestinal damage after methotrexate treatment of breast cancer in rats. *Dig Dis Sci* 47(12):2751–2757
- Gibson RJ, Keefe DM, Clarke JM, Regester GO, Thompson FM, Golland GJ, Edwards BG, Cummins AG (2002) The effect of keratinocyte growth factor on tumour growth and small intestinal mucositis after chemotherapy in the rat with breast cancer. *Cancer Chemother Pharmacol* 50(1):53–58. <https://doi.org/10.1007/s00280-002-0460-4>
- Bowen JM, Gibson RJ, Cummins AG, Tyskin A, Keefe DM (2007) Irinotecan changes gene expression in the small intestine of the rat with breast cancer. *Cancer Chemother Pharmacol* 59(3):337–348. <https://doi.org/10.1007/s00280-006-0275-9>
- Gibson RJ, Bowen JM, Keefe DM (2005) Palifermin reduces diarrhea and increases survival following irinotecan treatment in tumor-bearing DA rats. *Int J Cancer* 116(3):464–470. <https://doi.org/10.1002/ijc.21082>
- Barcelo A, Claustre J, Moro F, Chayvialle JA, Cuber JC, Plaisancie P (2000) Mucin secretion is modulated by luminal factors in the isolated vascularly perfused rat colon. *Gut* 46(2):218–224
- Ilg EC, Schafer BW, Heizmann CW (1996) Expression pattern of S100 calcium-binding proteins in human tumors. *Int J Cancer* 68(3):325–332. [https://doi.org/10.1002/\(sici\)1097-0215\(19961104\)68:3<325::aid-ijc10>3.0.co;2-7](https://doi.org/10.1002/(sici)1097-0215(19961104)68:3<325::aid-ijc10>3.0.co;2-7)
- Bowen JM, Gibson RJ, Keefe DM, Cummins AG (2005) Cytotoxic chemotherapy upregulates pro-apoptotic Bax and Bak in the small intestine of rats and humans. *Pathology* 37(1):56–62

33. Cohen J (2013) Statistical power analysis for the behavioral sciences. Taylor & Francis, New York
34. Logan RM, Gibson RJ, Bowen JM, Stringer AM, Sonis ST, Keefe DM (2008) Characterisation of mucosal changes in the alimentary tract following administration of irinotecan: implications for the pathobiology of mucositis. *Cancer Chemother Pharmacol* 62(1): 33–41. <https://doi.org/10.1007/s00280-007-0570-0>
35. Gibson RJ, Bowen JM, Inglis MR, Cummins AG, Keefe DM (2003) Irinotecan causes severe small intestinal damage, as well as colonic damage, in the rat with implanted breast cancer. *J Gastroenterol Hepatol* 18(9):1095–1100
36. Stringer AM, Gibson RJ, Bowen JM, Logan RM, Ashton K, Yeoh AS, Al-Dasooqi N, Keefe DM (2009) Irinotecan-induced mucositis manifesting as diarrhoea corresponds with an amended intestinal flora and mucin profile. *Int J Exp Pathol* 90(5):489–499. <https://doi.org/10.1111/j.1365-2613.2009.00671.x>
37. Takasuna K, Hagiwara T, Hirohashi M, Kato M, Nomura M, Nagai E, Yokoi T, Kamataki T (1996) Involvement of beta-glucuronidase in intestinal microflora in the intestinal toxicity of the antitumor camptothecin derivative irinotecan hydrochloride (CPT-11) in rats. *Cancer Res* 56(16):3752–3757
38. Takasuna K, Hagiwara T, Hirohashi M, Kato M, Nomura M, Nagai E, Yokoi T, Kamataki T (1998) Inhibition of intestinal microflora beta-glucuronidase modifies the distribution of the active metabolite of the antitumor agent, irinotecan hydrochloride (CPT-11) in rats. *Cancer Chemother Pharmacol* 42(4):280–286
39. Takasuna K, Hagiwara T, Watanabe K, Onose S, Yoshida S, Kumazawa E, Nagai E, Kamataki T (2006) Optimal anti-diarrhea treatment for antitumor agent irinotecan hydrochloride (CPT-11)-induced delayed diarrhea. *Cancer Chemother Pharmacol* 58(4): 494–503. <https://doi.org/10.1007/s00280-006-0187-8>
40. Cao XJ, Wang WM (2009) Histology and mucin histochemistry of the digestive tract of yellow catfish, *Pelteobagrus fulvidraco*. *Anat Histol Embryol* 38(4):254–261. <https://doi.org/10.1111/j.1439-0264.2009.00932.x>
41. Truter D, Strijdom H, Everson F, Kotze SH (2016) Mucin secreting cells in the stomach and colon are altered by combination antiretroviral treatment in an obese rat model. *Acta Histochem* 119:122–128. <https://doi.org/10.1016/j.acthis.2016.11.014>
42. Van Herreweghen F, Van den Abbeele P, De Mulder T, De Weirtd R, Geirmaert A, Hernandez-Sanabria E, Vilchez-Vargas R, Jauregui R, Pieper DH, Belzer C, De Vos WM, Van de Wiele T (2016) In vitro colonisation of the distal colon by *Akkermansia muciniphila* is largely mucin and pH dependent. *Benefic Microbes* 8:1–16. <https://doi.org/10.3920/bm2016.0013>
43. Laburthe M, Augeron C, Rouyer-Fessard C, Roumagnac I, Maoret JJ, Grasset E, Laboisse C (1989) Functional VIP receptors in the human mucus-secreting colonic epithelial cell line CL.16E. *Am J Phys* 256(3 Pt 1):G443–G450
44. Gutierrez MM, Alluisetti GB, Olabe JA, Amorebieta VT (2008) Nitrosation of N-methylhydroxylamine by nitroprusside. A kinetic and mechanistic study. *Dalton Trans* 37:5025–5030. <https://doi.org/10.1039/b805329d>
45. Phillips TE, Stanley CM, Wilson J (1993) The effect of 16,16-dimethyl prostaglandin E2 on proliferation of an intestinal goblet cell line and its synthesis and secretion of mucin glycoproteins. *Prostaglandins Leukot Essent Fat Acids* 48(6):423–428
46. Logan RM, Stringer AM, Bowen JM, Gibson RJ, Sonis ST, Keefe DM (2008) Serum levels of NFkappaB and pro-inflammatory cytokines following administration of mucotoxic drugs. *Cancer Biol Ther* 7(7):1139–1145
47. Specian RD, Neutra MR (1980) Mechanism of rapid mucus secretion in goblet cells stimulated by acetylcholine. *J Cell Biol* 85(3): 626–640
48. Specian RD, Neutra MR (1982) Regulation of intestinal goblet cell secretion. *Am J Phys* 242(4):G370–G379
49. Lake AM, Bloch KJ, Sinclair KJ, Walker WA (1980) Anaphylactic release of intestinal goblet cell mucus. *Immunology* 39(2):173–178
50. Deplancke B, Gaskins HR (2001) Microbial modulation of innate defense: goblet cells and the intestinal mucus layer. *Am J Clin Nutr* 73(6):1131s–1141s
51. Furness JB, Kunze WA, Clerc N (1999) Nutrient tasting and signaling mechanisms in the gut. II. The intestine as a sensory organ: neural, endocrine, and immune responses. *Am J Phys* 277(5 Pt 1): G922–G928
52. Furness JB (2012) The enteric nervous system and neurogastroenterology. *Nat Rev Gastroenterol Hepatol* 9(5):286–294. <https://doi.org/10.1038/nrgastro.2012.32>
53. McCool DJ, Marcon MA, Forstner JF, Forstner GG (1990) The T84 human colonic adenocarcinoma cell line produces mucin in culture and releases it in response to various secretagogues. *Biochem J* 267(2):491–500
54. Turner JE, Stockinger B, Helmby H (2013) IL-22 mediates goblet cell hyperplasia and worm expulsion in intestinal helminth infection. *PLoS Pathog* 9(10):e1003698. <https://doi.org/10.1371/journal.ppat.1003698>
55. Sultani M, Stringer AM, Bowen JM, Gibson RJ (2012) Anti-inflammatory cytokines: important immunoregulatory factors contributing to chemotherapy-induced gastrointestinal mucositis. *Chemother Res Pract* 2012:490804–490811. <https://doi.org/10.1155/2012/490804>

**Publisher's Note** Springer Nature remains neutral with regard to jurisdictional claims in published maps and institutional affiliations.